

Modulated photothermal radiometry for thermal diffusivity measurement and layer surface characterization

by S. Pham Tu Quoc, G. Cheymol, A. Semerok

CEA Saclay, DEN/DANS/DPC/SEARS/LISL, 91191 Gif sur Yvette, France, sang.phamtuquoc@cea.fr; guy.cheymol@cea.fr; alexandre.semerok@cea.fr

Abstract

A new method relying on modulated photothermal radiometry with laser heating is presented for characterization of the thickness and the thermal diffusivity of materials. This non-destructive and contactless method is based on phase shift measurement between modulated laser power and thermal signal at different modulation frequencies. New simple formulas were found for thickness and thermal diffusivity determination for metal samples. The experimental setup is presented. Layer on substrate is studied with theoretical 3D-model developed in our laboratory. First measurements on virgin and oxidized nuclear fuel cladding are presented.

1. Introduction

This paper presents a new method of the modulated photothermal radiometry¹ (PTR) technique for characterizing the thermal properties of a plate and a layer on substrate. The PTR is a non-destructive and contactless technique for the characterization of materials which has two major advantages: good signal-to-noise ratio through a synchronous detection and independence on the heating power and the optical properties of the sample surface. The principle of the PTR consists in heating a sample with a modulated light power and then observing the emitted infrared radiation. In the stationary regime of the heating, the thermal response can be described as a modulated signal giving the amplitude and the phase shift -versus the laser modulation- of the temperature. Knowing the phase shift and the temperature amplitude at different frequencies permits to characterize the sample by fitting the theoretical results. The phase shift has several advantages over the temperature amplitude such as it is independent of the sample's reflectivity and the light power^{2,3}. Nowadays, there are several methods to measure these parameters but each one has its disadvantages: can only be applied to bulk materials^{4,5,6}, requires use of a small focused beam⁷ and requires the variation of the sample surface temperature which can be influenced by the heat loss effect⁸.

Our concern is to obtain firstly remote and contactless measurements with one face access and secondly, simple methods with acceptable performance in order to measure in-situ the variation of the thermal properties of nuclear components. The method presented is based on a model of the laser heating of a sample⁹ that gives an analytical expression for the amplitudes and phases of the sample surface temperature with constant optical and thermo-physical parameters during the laser heating. Through sensitivity analysis and multi-parameter analysis, simple formulas were obtained to determine the thermal properties of a plate or a layer on substrate.

2. 3D thermal model of the modulated laser heating for layer on substrate

Below is presented the thermal model for the laser heating of a layer on semi-infinite substrate. The variation of optical and thermal properties with temperature, the surface roughness and the heat exchange by convection between the sample surfaces and the air are supposed to be negligible. The layer is supposed to be opaque in laser wavelength which means that the laser photons are only absorbed at a shallow depth. By applying the Fourier series analysis to the intensity of the laser beam and the temperature in the stationary regime of the laser heating⁹, the complex temperature amplitude at the heating center of the front face can be written as:

$$\Delta\tilde{T} = -\frac{\alpha_l(1-R_l)iI_0}{k_l} \int_0^{+\infty} \frac{\Theta(\xi)}{\sigma_l^2 - \alpha_l^2} \left(\frac{2\alpha_l e^{-\sigma_l L} \Omega}{\sigma_l \Psi} + 1 - \frac{\alpha_l}{\sigma_l} \right) d\xi \quad (1)$$

$$\Omega = \left(e^{-\alpha_l L} - e^{-\sigma_l L} \right) (1 + k_s \sigma_s R) + \left(e^{-\sigma_l L} - \frac{\sigma_l}{\alpha_l} e^{-\alpha_l L} \right) \frac{k_s \sigma_s}{k_l \sigma_l}; \quad \Psi = \left(1 + e^{-2\sigma_l L} \right) \frac{k_s \sigma_s}{k_l \sigma_l} + \left(1 - e^{-2\sigma_l L} \right) (1 + k_s \sigma_s R)$$

$$\sigma_l = \sqrt{\xi^2 - \frac{2\pi f \rho_l C_l}{k_l}}; \quad \sigma_s = \sqrt{\xi^2 - \frac{2\pi f \rho_s C_s}{k_s}}; \quad \Theta(\xi) = \frac{\xi r_0^2}{2} \exp\left(-\frac{\xi^2 r_0^2}{4}\right) \text{ for a Gaussian beam}$$

ρ_l , C_l , k_l and ρ_s , C_s , k_s are respectively density, mass-specific heat and thermal conductivity of the layer and the substrate; L is the layer thickness; α_l and R_l are respectively the laser absorption coefficient and the reflectivity of the layer; R is the thermal resistance between layer and substrate; r_0 and l_0 are respectively the laser beam radius at $1/e$

intensity and the mean intensity of the Gaussian laser beam; f , t and i are respectively the repetitive rate frequency of the laser, the time and the complex unity; ξ and J_0 are respectively the variables of integration and the zero order Bessel functions of the first kind.

The phase shift between the laser and the thermal response of the front surface can be described as:

$$\Delta\Phi = a \tan\left(\frac{\text{Re}al(\Delta\tilde{T})}{\text{Im}ag(\Delta\tilde{T})}\right) \quad (2)$$

This model can be used to fit the theoretical phase-shift to the experimental results in order to characterize the layer thickness and its thermal properties. Our objective is to develop a simple characterization method with good precision. We thus performed multi-parametric modeling to determine the dependence of particular points in the phase-shift vs. frequency curve which can provide us with simple relations between different parameters.

3. Multi-parametric modeling of the phase shift for a plate

Firstly, the simple sample without substrate was studied. In order to obtain the analytical expression of laser plate heating, the thermal resistance R in equation (1) between layer and substrate was supposed infinite and the substrate is replaced by the air. We successively analyzed, one at a time, the influence of different interactions and plate parameters on the phase shift, including: absorption coefficient α , thermal conductivity k , volumetric specific heat ρC_v , laser beam radius r_0 and thickness L . We used the sensitivity coefficient⁴ $S_x = x \frac{\partial \Delta\Phi}{\partial x}$ for this analysis; the results are presented in figure 1:

According to the sensitivity analysis results, the following was concluded with regard to the influence of the different parameters on the phase shift:

- The influence of the absorption coefficient α is negligible for opaque sample.
- The sensitivity of the thermal conductivity and the volumetric specific heat are equivalent for all frequency. This means that the thermal conductivity and volumetric specific heat influence the phase shift by their ratio k/C_v (thermal diffusivity D).
- The sensitivity to the thermal properties is zero at the minimal phase shift Φ_{min} ; that means that the minimal phase shift is independent from the thermal properties.

We plotted the minimum phase shift as a function of the layer thickness and the laser beam radius and we used the numerical regression to determine the relation (3) between the layer thickness $L(m)$, the laser beam radius $r_0(m)$ and the minimum phase shift $\Phi_{min}(^\circ)$.

$$L = \frac{1}{1.5} r_0 \ln\left(\frac{90}{|\Phi_{min}|}\right) \quad \text{with } 2L < r_0 < 100L \quad (3)$$

While the minimum phase shift does not render it possible to determine the thermal properties, since it only varies with the thickness and the beam radius, according to (3), the frequency of the minimum phase shift varies linearly with the thermal diffusivity, cf. figure 2, and could provide us with information about the thermal diffusivity.

$$k=13\text{Wm}^{-1}\text{K}^{-1}, C_v=3.7\text{MJ}\text{K}^{-1}\text{m}^{-3}, L=100\mu\text{m}, r_0=1740\mu\text{m}, \alpha=20\mu\text{m}^{-1}.$$

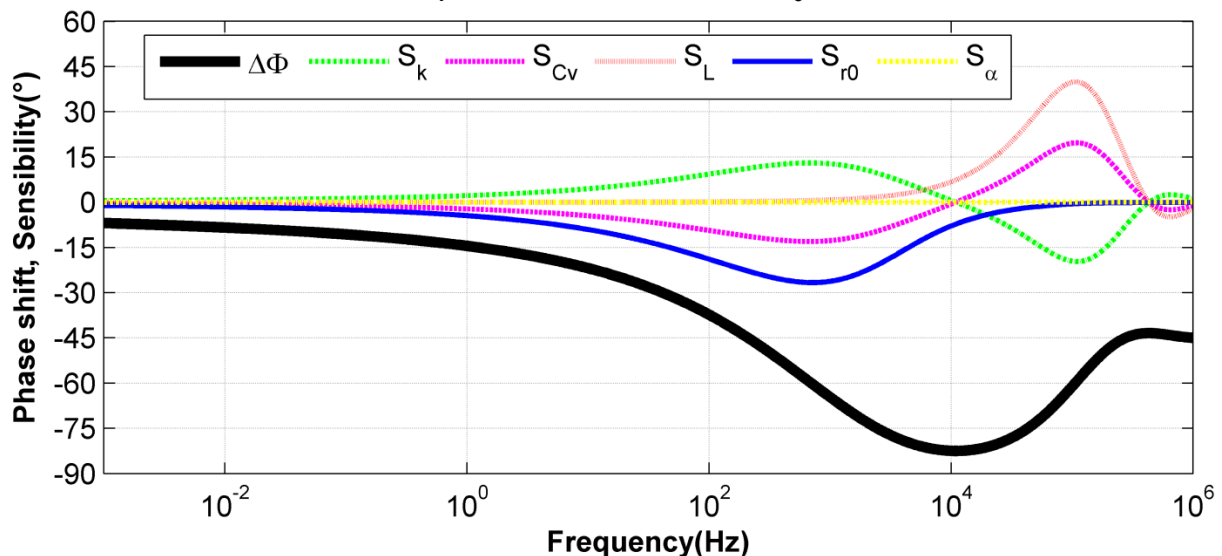


Fig. 1. Phase shift ($\Delta\Phi$) at the beam centre and sensibility of $\Delta\phi$ to thermal conductivity (S_k), mass-specific heat (S_{Cv}), thickness (S_L), laser beam radius (S_{r0}) and absorption coefficient (S_α) of a homogeneous plate

We plotted the frequency of the minimum phase shift as a function of the plate thickness and the laser beam radius. By using the numerical regression, the thermal diffusivity can be determined with the follow formula:

$$D = \alpha_{r_0/L} f_{min} L r_0 \quad \text{with } 2L < r_0 < 100L \quad (4)$$

where f_{min} in Hz, L in m, D in m^2/s , r_0 in m, and where $\alpha_{r_0/L}$ depends on the ratio r_0/L . Numerical calculations were performed for $\alpha_{r_0/L}$ and the results of $\alpha_{r_0/L}$ are presented in figure 3. The laser beam radius is limited in the range $2L < r_0 < 100L$ so that the minimum phase shift is well defined.

We then have two simple formulas giving the sample thickness (Eq. 3) and the thermal diffusivity (Eq. 4) by knowing the minimum phase shift and the related frequency.

4. Multi-parametric modeling of the phase shift for a layer on semi-infinite substrate

When the thermal resistance between the layer and the substrate goes to infinite ($R=\infty$), the influence of the substrate is negligible and the results of the phase shift is the same as a plate. We now analyse two another cases for $R=0$ and $R\neq 0$

4.1. Thermally perfect contact between layer and substrate ($R=0$) and $L \ll r_0$

The thermal resistance R in equation (1) between layer and substrate is considered equal to zero. We are interested in thin layer deposited over a substrate for protection or the oxide layer appearing over the nuclear components. The sensitivity analysis is presented in figure 4 for thin layer of graphite ($L \ll r_0$) on substrate of copper. The layer is considered opaque and absorbent.

At the red cross position in figure 4, the sensitivity of the layer thickness, the laser beam radius, the absorption coefficient and the thermal diffusivity (k/C_v) of the layer and the substrate is zero, there is only the influence of the thermal effusivity ($\sqrt{k.C_v}$). The influence of the thermal effusivity of the layer and the substrate is equivalent at all frequency that signifies their influences were affected by the ratio E_c/E_s . The red cross position was defined by the first extremal phase shift if the minimum phase shift is inferior to -45° and by the second extremal phase shift if the minimum phase shift is superior to -45° (cf. figure 5). The phase shift at this extremal position can provide the value of the ratio E_c/E_s .

In order to determine the relation between the ratio E_c/E_s and the extremal phase shift, we plotted the phase shift as a function of the frequency for different ratio E_c/E_s in figure 5, then the ratio E_c/E_s as fonction of the extremal phase shift in figure 6. By using the numerical regression, the relation between the E_c/E_s and the extremal phase shift was determined with the follow formula:

$$\frac{E_c}{E_s} = -(\tan(\Phi_{extremal}))^{1.5} \quad (5)$$

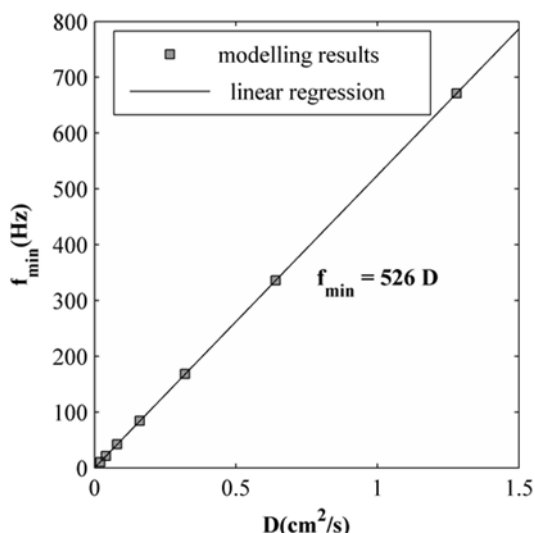


Fig. 2. Frequency f_{min} as a function of the thermal diffusivity. Laser beam radius $r_0=1\text{mm}$ and layer thickness $L=100\mu\text{m}$

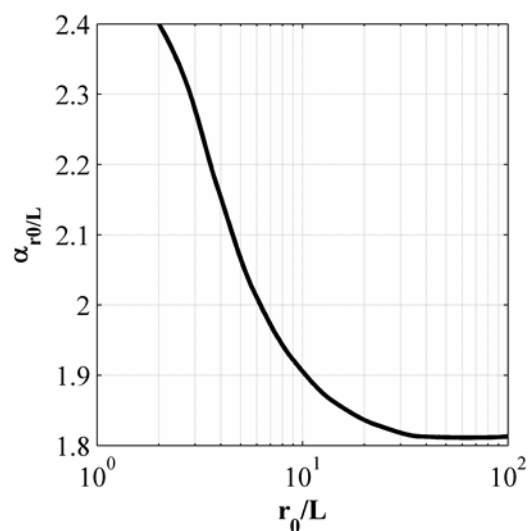


Fig. 3. Values of $\alpha_{r_0/L}$ for different values of the r_0/L ratio

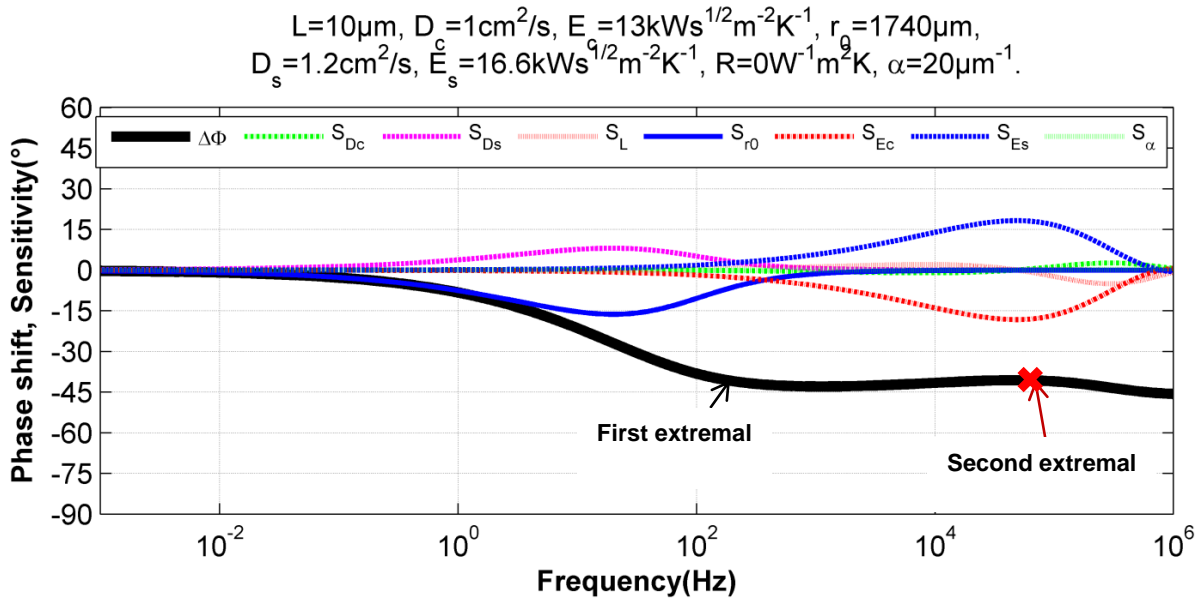


Fig. 4. Phase shift ($\Delta\Phi$) at the beam centre and sensitivity of $\Delta\phi$ to thermal diffusivity (S_{Dc} , S_{Ds}), thermal effusivity (S_{Ec} , S_{Es}), layer thickness (S_L), laser beam radius (S_{r0}) and absorption coefficient (S_α) of graphite on copper

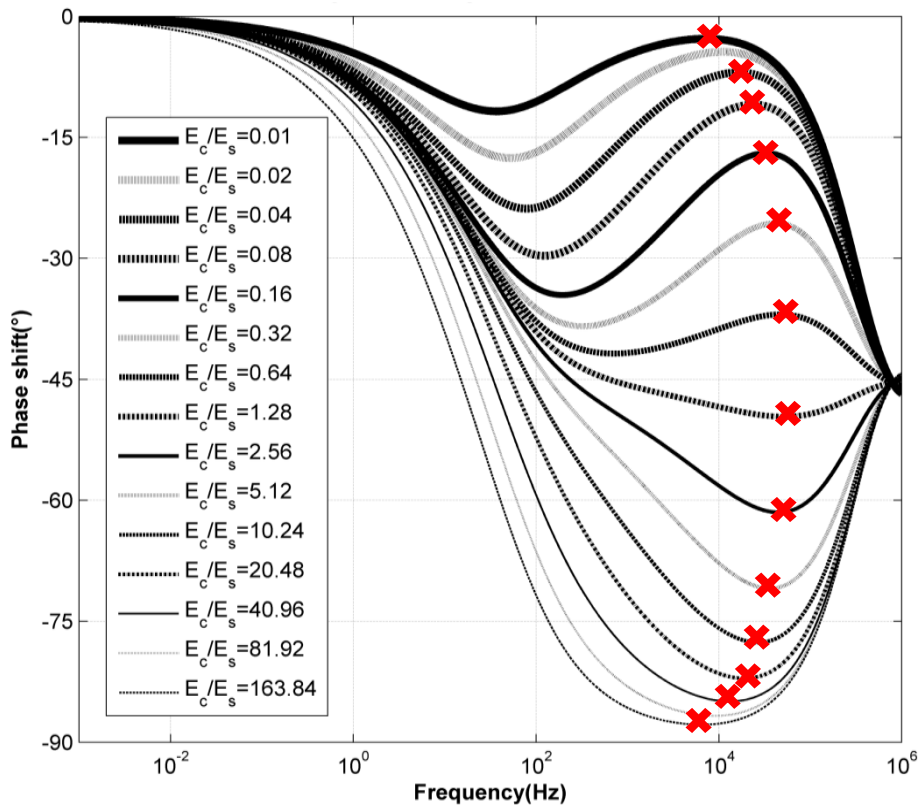


Fig. 5. Phase shift as a function of the frequency for different value of E_c/E_s . $r_0=1740\mu\text{m}$, $L=10\mu\text{m}$

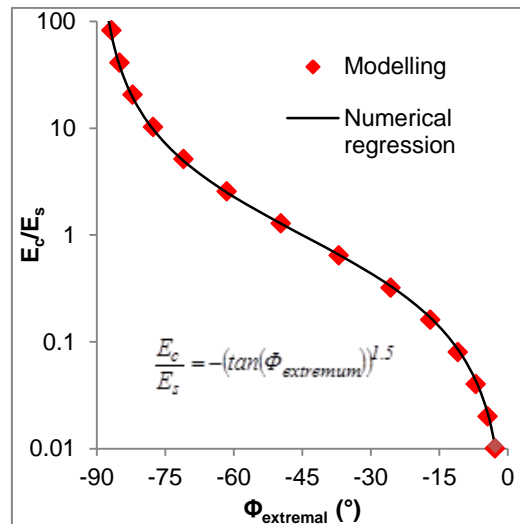


Fig. 6. Ratio E_c/E_s as a function of the extremal phase shift

4.2. Thermally intermediate contact between layer and substrate ($R \neq 0$) and $L \gg r_0$

If the thermal resistance is different to zero, the sensitivity analysis shows that the influences of parameters are very complicated. In this paper, we only present the results for the laser beam radius much smaller than the layer thickness ($L \gg r_0$). The sensitivity analysis in figure 7 shows that only two parameters influence the phase shift: the thermal diffusivity of the layer and the laser beam radius. The maxima sensibility is in the slope of the phase shift curve or in the phase shift $-22,5^\circ$. We plotted the phase shift as function of the frequency for different values of D_c and r_0 , then the frequency at phase shift $-22,5^\circ$ as function of D_c and r_0 in figure 8. By the numerical regression, we determined the relation between the thermal diffusivity of the layer D_c , the laser beam radius r_0 and the frequency at $-22,5^\circ$ $f_{-22,5^\circ}$

$$D_c = 3.5 f_{-22,5^\circ} \cdot r_0^2 \quad \text{with } L \ll r_0 \quad (6)$$

where $f_{-22,5^\circ}$ in Hz, D_c in m^2/s , r_0 in m

$$L=1000\mu\text{m}, D=0.25\text{cm}^2/\text{s}, E=11.5\text{kWs}^{1/2}\text{m}^{-2}\text{K}^{-1}, r_0=100\mu\text{m},$$

$$D_s=0.038\text{cm}^2/\text{s}, E_s=7\text{kWs}^{1/2}\text{m}^{-2}\text{K}^{-1}, R=1\text{E-}004\text{W}^{-1}\text{m}^2\text{K}, \alpha=20\mu\text{m}^{-1}.$$

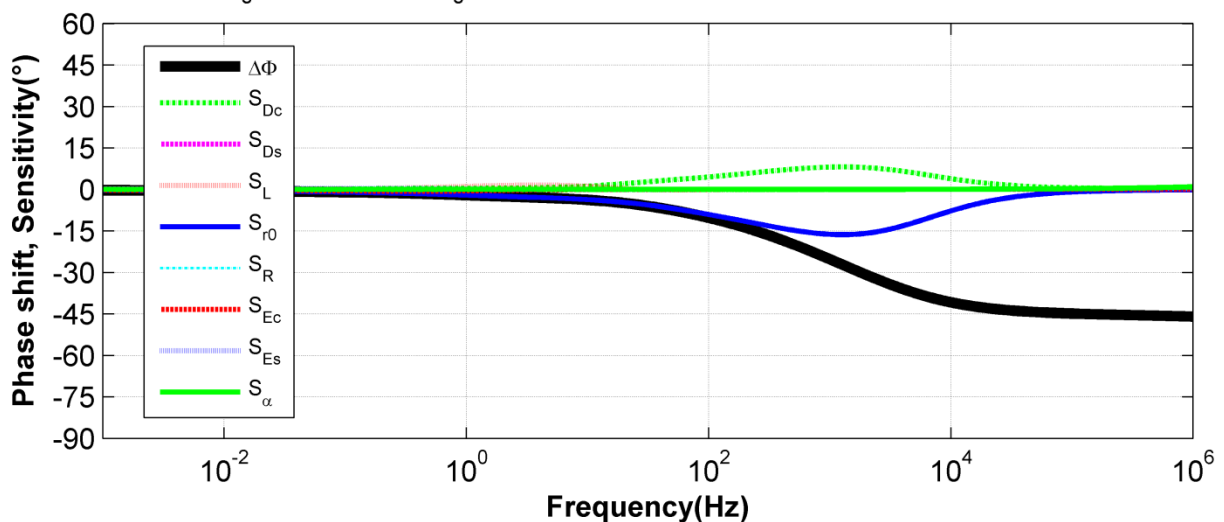


Fig. 7. Phase shift ($\Delta\Phi$) at the beam centre and sensitivity of $\Delta\phi$ to thermal diffusivity (S_{Dc} , S_{Ds}), thermal effusivity (S_{Ec} , S_{Es}), layer thickness (S_L), laser beam radius (S_{R0}), thermal resistance (S_R) and absorption coefficient (S_α) of tantalum on stainless steel.

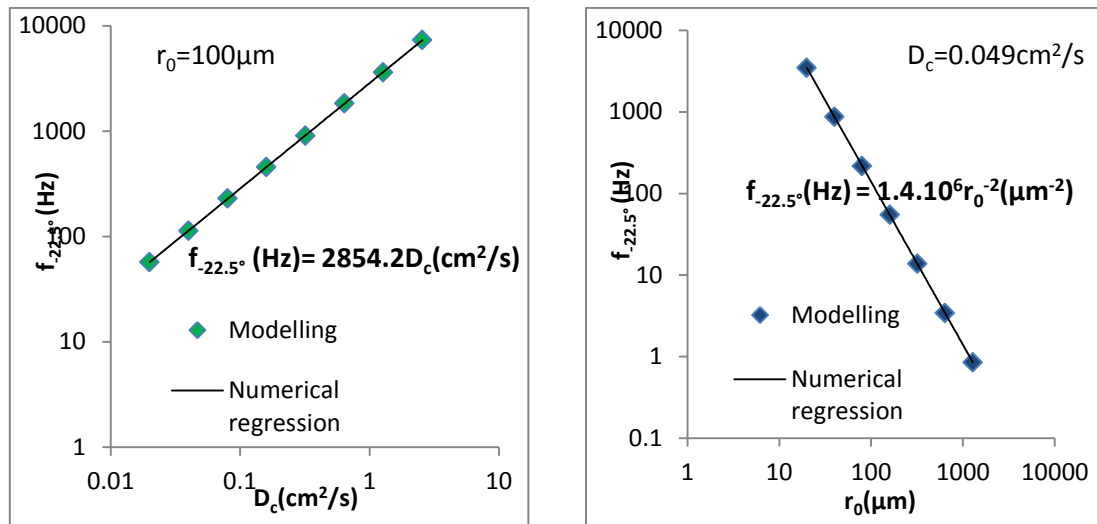


Fig. 8. Frequency at phase shift -22.5° as function of D_c and r_0 . Laser beam radius $r_0=100\mu\text{m}$

5. Experimental setup

The schema for the experimental set up is presented in figure 9. We used the fiber laser MANLIGHT ML50-CW-R-TKS to heat the sample with an average power from 5W to 10W. The beam radius r_0 was $1740\mu\text{m}$ (radius at 1/e intensity) and the wavelength λ was 1080nm . The laser beam was guided to the sample by a beam splitter with 99% power transmission, and the 1% reflected laser power was collected by a photodiode. The thermal flux of the sample was measured by an IR detector VIGO PVMI-3TE-10.6 with a useful spectral range λ from $2\mu\text{m}$ to $10\mu\text{m}$ and a sensitive area of 1mm^2 . The thermal flux was focused on the IR detector by a ZnSe convex lens. In order to avoid that the diffuse reflection of the laser entered the detector center (there is low sensitivity on $1\mu\text{m}$ wavelength), a Germanium filter was positioned in front of the detector. Thus, only wavelengths ranging between $2\mu\text{m}$ and $14\mu\text{m}$ were transmitted. We used the lock-in amplifier SR530 to determine the phase shift between the laser power signal and the thermal signal.

Our detector best performs in the spectral range from $6\mu\text{m}$ to $8\mu\text{m}$, therefore we chose to heat the sample around $400\text{K} \pm 50\text{K}$. The temperature amplitude in the stationary regime was inferior to 10K and the thermal properties could thus be considered constant during the heating. The IR detector was set to receive the thermal flux coming from the center of the heating on the sample surface.

In our method, the accuracy of the measurement of the phase shift and modulation frequency is important to determine the frequency at the minimum phase shift with high accuracy. In order to measure the phase shift $\Delta\varphi_{\text{thermal-laser}}$ between the laser power and the thermal signal, we measured firstly the phase-shift $\Delta\varphi_1$ between the signal of the electric generator and the thermal signal detected by the IR detector $\Delta\varphi_1 = \Delta\varphi_{\text{thermal-laser}} + \Delta\varphi_{\text{laser}} + \Delta\varphi_{\text{IR detector}} + \Delta\varphi_{\text{lock-in}}$, where $\Delta\varphi_{\text{laser}}$, $\Delta\varphi_{\text{IR detector}}$ and $\Delta\varphi_{\text{lock-in}}$ are, respectively, the internal phase shifts of the laser, the IR detector and the lock-in amplifier. Secondly, the phase-shift $\Delta\varphi_2$ between the signal of the electric generator and the laser power detected by the photodiode $\Delta\varphi_2 = \Delta\varphi_{\text{laser}} + \Delta\varphi_{\text{photodiode}} + \Delta\varphi_{\text{lock-in}}$, where $\Delta\varphi_{\text{photodiode}}$ is the internal phase shift of the photodiode. The phase shift $\Delta\varphi_{\text{thermal-laser}}$ was $\Delta\varphi_{\text{thermal-laser}} = \Delta\varphi_1 - \Delta\varphi_2 - \Delta\varphi_{\text{IR detector}} + \Delta\varphi_{\text{photodiode}}$. The phase shift $\Delta\varphi_{\text{photodiode}} - \Delta\varphi_{\text{IR detector}}$ was measured by using a chopper (Stanford SR540) and the laser in continuous regime. We measured the phase shift $\Delta\varphi_3$ between the chopper and the photodiode $\Delta\varphi_3 = \Delta\varphi_{\text{chopper}} + \Delta\varphi_{\text{photodiode}} + \Delta\varphi_{\text{lock-in}}$ and the phase shift $\Delta\varphi_4$ between the chopper and the IR detector (without germanium filter) $\Delta\varphi_4 = \Delta\varphi_{\text{chopper}} + \Delta\varphi_{\text{IR detector}} + \Delta\varphi_{\text{lock-in}}$, where $\Delta\varphi_{\text{chopper}}$ is the internal phase shift of the chopper. Finally we had $\Delta\varphi_{\text{thermal-laser}} = \Delta\varphi_1 - \Delta\varphi_2 + \Delta\varphi_3 - \Delta\varphi_4$ with all internal phase shifts of the instrument included. The final accuracy of the phase shift measurement was $\approx 98\%$. The frequency of the electric generator was measured by the lock-in amplifier with $\approx 99.5\%$ accuracy.

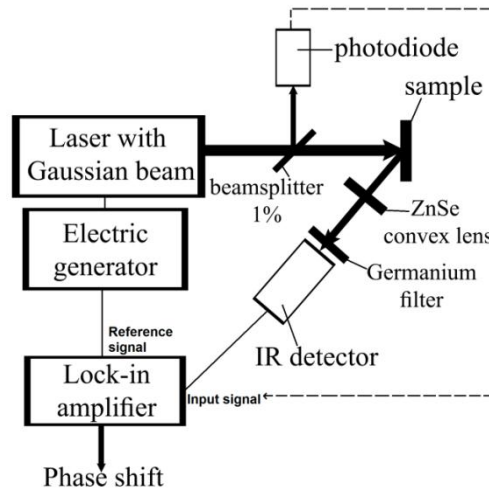


Fig. 9. Scheme of the experimental setup

6. Experimental results

6.1. The plate thickness and the thermal diffusivity measurement by using equation (3) and (4)

In this paper we present the results by using the equations (3) and (4). The modelling result of (5) shows interest for characterisation of thin layer on substrate and equation (6) can be used to characterize the thermal diffusivity of thick layer on substrate.

Figures 10 (a-d) present the experimental results of the phase shift as a function of frequency for different materials: 304L Stainless Steel, Nickel, Titanium, Tungsten, Molybdenum, Iron, and Zinc. From the figures, the minimum phase shift Φ_{min} and its frequency f_{min} were determined. Subsequently, the thickness and the thermal diffusivity were calculated by using Equation (3) and (4) and are presented in Table I (L_c and D_c).

Table I shows that the samples thickness L_m obtained by Equation (3) corresponded to the values L_c measured by the height gauge TESA-HITE 400. The accuracy of L_m was higher than that of L_c but the advantage of L_c measurements is the fact that the measurements were contactless.

The measured values of both D_m and D_c correspond quite well to the reference values D_{ref} . The incertitude of D_m ranges from 5% to 10%, that of D_c from 10% to 15%. The incertitude of D_c and D_m depended mainly on the precision of the determination of the frequency f_{min} at the minimum phase-shift. The accuracy of D_m was higher than that of D_c because of the precision of the sample thickness measurement. While D_c was obtained by a contactless measurement of L , the values of D_m had to be measured with a contact measurement of L . Most of the thermal diffusivity results were underestimated with the reference values; this could be caused by an underestimation of f_{min} . It should also be noted that the reference values depend on the temperature and the chemical composition or purity of the sample. We are working on the optimization of the determination of f_{min} and the temperature measurement to increase the accuracy of the results.

6.2. The thickness and thermal diffusivity measurement of fuel cladding

Then three samples of cylindrical fuel cladding with thickness $570\mu\text{m}$ and external radius 9.5mm have been tested. The first sample is the original fuel cladding without oxide layer. The second and the third sample are respectively with $5\mu\text{m}$ and $10\mu\text{m}$ oxide layer ZrO_2 . The oxide layer was prepared in an oven with temperature 500°C under air. The sample with $10\mu\text{m}$ oxide layer has a small nitriding surface because of the time heating in the oven. The results of the phase shift are presented in figure 11.

Figure 11 shows that the phase shift at low frequency has a very little influence by the oxide layer. The phase shift at low frequency is almost the same for three samples and can be used to determine the thickness and the thermal diffusivity of the Zircaloy 4 by the equation (3) and (4), the results are presented in table 2.

At high frequency, there is various phase shifts for two thicknesses of the oxide layer ZrO_2 ($5\mu\text{m}$, $10\mu\text{m}$). The thicker the oxide layer, the more the phase shift curve decreases rapidly. These preliminary results are very encouraging and allow considering the possibility of determination the thickness of the ZrO_2 oxide layer by a non-contact measurement and distance, but our model can't be used without modification since the substrate is semi-infinite and the layer is opaque in our model.

7. Conclusion

We have herein proposed and validated a new method for measuring the thermal diffusivity of a plate. When the plate thickness and the minimum phase shift between the laser and the thermal response of the front face are known, the thermal diffusivity can be determined. This method is applicable to opaque plate with a thickness L much larger than the laser absorption length $1/\alpha$ and L much smaller than the plate dimensions. The laser beam radius must be in the range $2L \leq r_0 \leq 100L$.

Our results on the measurements of the thickness and the thermal diffusivity of Zircaloy 4 cladding were close to the reference values. The difference between the reference and experimental results may be due to the cylindrical shape of the sample surface, while the equations (3) and (4) were determined for flat surfaces. The model or experimental configuration can be modified to ensure better accuracy of determination.

Such PTR method can be used to determine the thicknesses and thermo-physical properties of plates and tubes, to detect the defects of the components and also to measure their variations in time. This method has several advantages: the process and experimental setup are simple; the phase shift does not depend on the laser power or the optical properties of the surface. The understanding of the thermal diffusivity behavior in time, at various temperatures and in severe environments helps to determine the lifetime of components and astutely choose materials for design and construction.

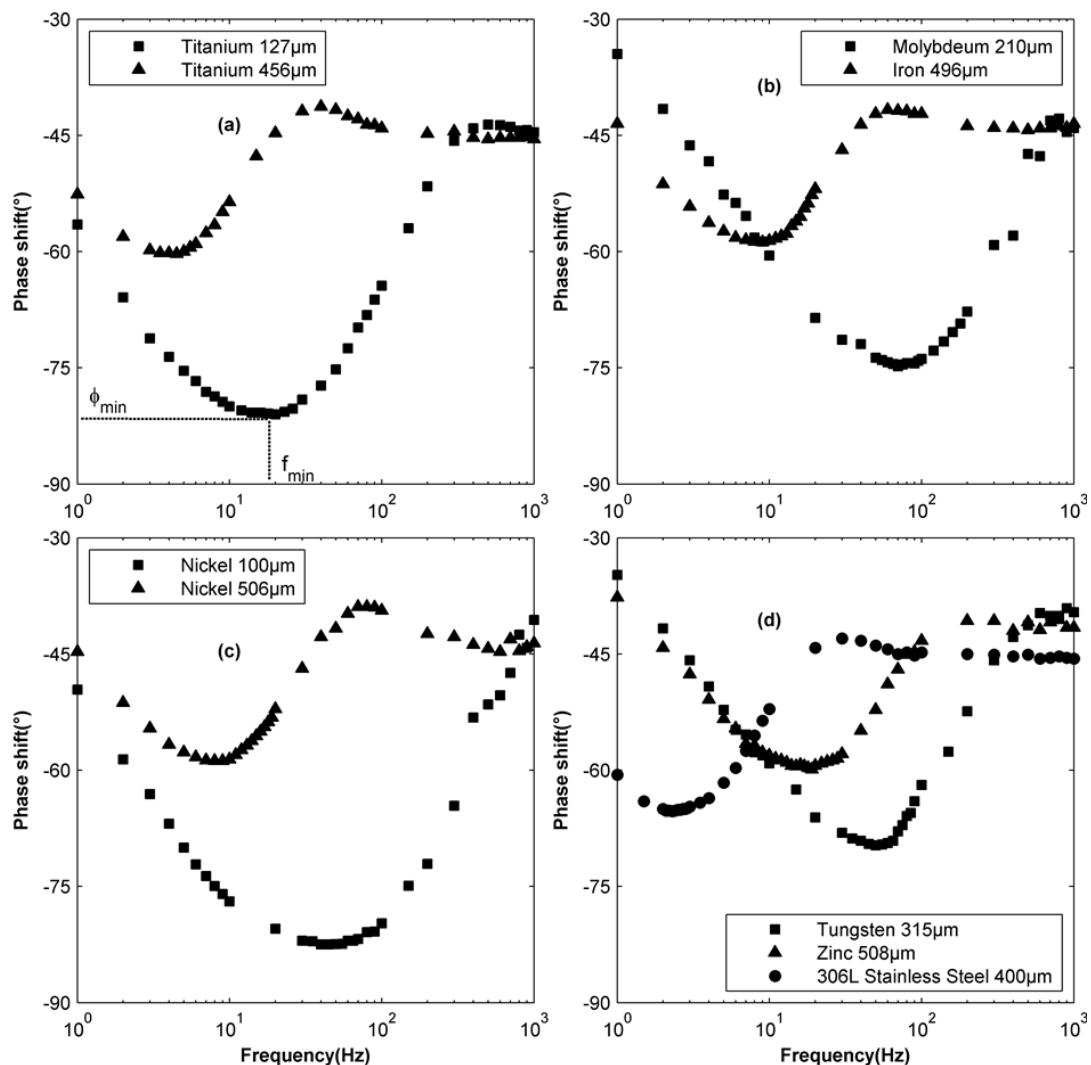


Fig. 10. Phase shift as a function of frequency for nickel, tungsten, zinc, 304L stainless steel, titanium, molybdenum and iron. The incertitude of the phase shift was $\pm 1^\circ$; the incertitude of the frequency was $\pm 0.5\%$. Laser beam radius $r_0=1740\mu\text{m}$

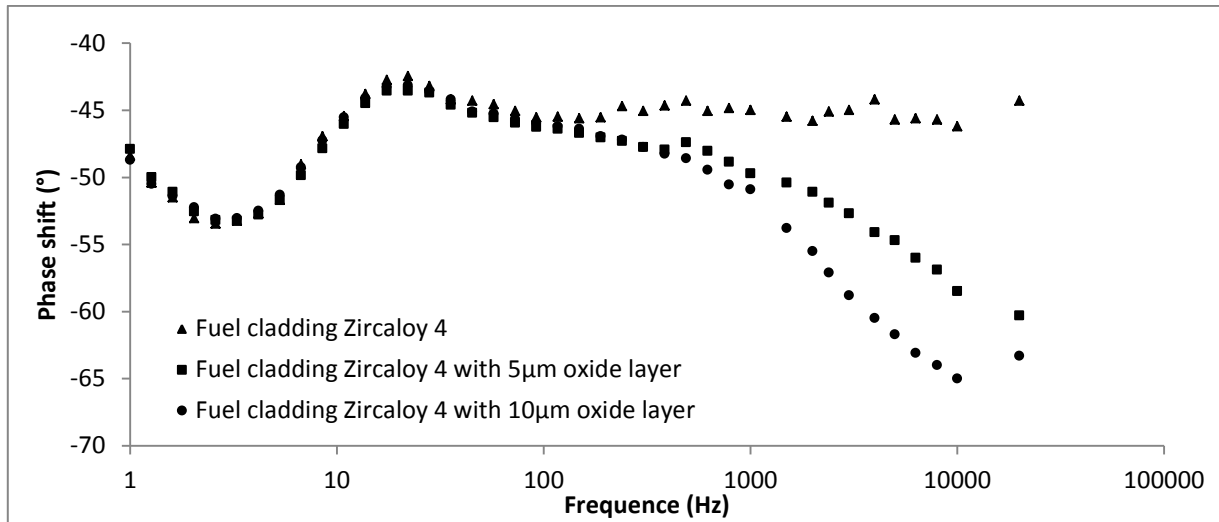


Fig. 11. Phase shift as a function of frequency for fuel cladding. The incertitude of the phase shift was $\pm 1^\circ$; the incertitude of the frequency was $\pm 0.5\%$. Laser beam radius $r_0=1740\mu\text{m}$

Table 1. Heating parameters and thermal diffusivity measured for 304L Stainless Steel, Nickel, Titanium, Tungsten, Molybdenum, Iron and Zinc. Comparison with reference values¹⁰

	Titanium 127µm	Titanium 456µm	Iron 496µm	Molybdenum 210µm	Nickel 100µm	Nickel 506µm	Tungsten 315µm	Zinc 508µm	304L Stainless Steel 400µm
T (K) ^a	400 ± 5	410 ± 5	370 ± 5	360 ± 5	410 ± 5	350 ± 5	350 ± 5	370 ± 5	450 ± 5
$r_0(\mu\text{m})$ ^b	1740 ± 30								
$\Phi_{min}(^\circ)$ ^c	-81 ± 1	-60.3 ± 1	-58.8 ± 1	-74.8 ± 1	-82.5 ± 1	-58.8 ± 1	-69.5 ± 1	-59.2 ± 1	-64.8 ± 1
$f_{min}(\text{Hz})$ ^d	18.5 ± 2	4.25 ± 0.5	9 ± 1	77.5 ± 10	50 ± 5	9 ± 1	55 ± 5	19 ± 2	2.5 ± 0.3
$L_m(\mu\text{m})$ ^e	127 ± 2.5	456 ± 2.5	496 ± 2.5	210 ± 2.5	100 ± 2.5	506 ± 2.5	315 ± 2.5	508 ± 2.5	400 ± 2.5
$L_c(\mu\text{m})$ ^f	119 ± 14	456 ± 22	488 ± 23	206 ± 15	98 ± 13	487 ± 23	296 ± 17	494 ± 21	385 ± 19
D_m (cm^2/s) ^g	0.076 ± 0.008	0.073 ± 0.007	0.171 ± 0.016	0.538 ± 0.068	0.177 ± 0.016	0.174 ± 0.016	0.618 ± 0.052	0.369 ± 0.033	0.037 ± 0.004
D_c (cm^2/s) ^k	0.071 ± 0.011	0.073 ± 0.008	0.168 ± 0.017	0.528 ± 0.077	0.159 ± 0.027	0.168 ± 0.017	0.538 ± 0.057	0.359 ± 0.034	0.034 ± 0.004
D_{ref} (cm^2/s) ^l	0.082 ± 0.008	0.081 ± 0.008	0.191 ± 0.019	0.520 ± 0.052	0.185 ± 0.018	0.204 ± 0.020	0.626 ± 0.062	0.395 ± 0.039	0.039 ± 0.004

^a T : temperature measured by thermocouple.
^b r_0 : laser beam radius measured by CCD camera.
^c Φ_{min} : minimum phase shift ϕ_{min} measured on the phase shift curve.
^d f_{min} : frequency f_{min} measured by a numerical algorithm.
^e L_m : plate thickness measured by height gauge TESA-HITE 400.
^f L_c : plate thickness calculated with Equation (3).
^g D_m : thermal diffusivity measured by Equation (4) with L_m .
^k D_c : thermal diffusivity measured by Equation (4) with L_c .
^l D_{ref} : thermal diffusivity reference¹⁰ at temperature T(K).

Table 2. Thickness and thermal diffusivity measurement of fuel cladding Zircaloy 4.
Measured by equation (3) and (4)

	Cladding Zy4	Cladding Zy4 with 5µm oxide layer	Cladding Zy4 with 10µm oxide layer	Reference	Accuracy
Φ_{min}	-53.5°	-53.3°	-53.1°		
f_{min}	3.11 Hz	3.11 Hz	3.11 Hz		
Thickness	603 µm	608 µm	612	570 µm	6-7%
Thermal diffusivity	0.075 cm ² /s	0.076 cm ² /s	0.076 cm ² /s	0.072 cm ² /s	4-6%

REFERENCES

- [1] O. Breitenstein and M. Langenkamp, *Lock-in Thermography* (Springer, Berlin, 2003).
- [2] A. Rosencwaig and J. B. Willis, *Journal of Applied Physics* **51**, 4361 (1980).
- [3] G. Busse, *Applied Optics*, **21**, 107 (1982).
- [4] G. Rousset et F. Lepoutre, *Revue Phys. Appl.* **17**, 201 (1982).
- [5] A. Salazar, A. Stinchez-Lavega, and J. Fernandez, *Journal of Applied Physics*, **69**, 1216 (1991).
- [6] L. Fabbri et al., *Rev. Sci. Instrum.* **66**, 3593 (1995).
- [7] Arantza Mendioroz, Raquel Fuente-Dacal, Estibaliz Apiñaniz, and Agustín Salazar, *Rev. Sci. Instrum.* **80**, 074904 (2009).
- [8] Agustín Salazar, Arantza Mendioroz, and Raquel Fuente, *Applied Physics Letters*, **95**, 121905 (2009).
- [9] A. Semerok, F. Jaubert, S. Fomichev, P.-Y. Thro, X. Courtois, Ch. Grisolia, *Nuclear Instruments and Methods in Physics Research A*, **693**, 98 (2012).
- [10] Y. S. Touloukian, R. W. Powell, C. Y. Ho, M. C. Nicolaou, *Thermal diffusivity* (IFI/Plenum, New York, 1973).